DALTON

# Crystal structure, magnetic properties and spectroscopic studies of bis[1,3-bis(pyrazol-3-yl)triazenido]dicopper(II) trihydrate: a dinuclear complex with an asymmetric double pyrazolate bridge

**Vincent P. Hanot,[a] Toussaint D. Robert,*[,a] Jeroen Kolnaar,[b] Jaap G. Haasnoot,[b] Jan Reedijk,[b] Huub Kooijman[c] and Anthony L. Spek †[,c]**

[a] *Department of General Chemistry, Faculty of Medicine, University of Mons-Hainaut, Place du Parc, 20, B-7000 Mons, Belgium*
[b] *Leiden Institute of Chemistry, Gorlaeus Laboratories, Leiden University, PO Box 9502, 2300 RA Leiden, The Netherlands*
[c] *Department of Crystal and Structural Chemistry, Bijvoet Center for Biomolecular Research, Utrecht University, Padualaan, 8, 3584 CH Utrecht, The Netherlands*

The crystal and molecular structure of $[\{Cu(bpzt)\}_2]\cdot 3H_2O$ [$H_2bpzt$ = 1,3-bis(pyrazol-3-yl)triazene] was determined by X-ray diffraction methods. The complex has a quasi-planar dinuclear structure with an asymmetric double pyrazolate bridge. The asymmetry results from the presence, on the $C^3$ of each bridging pyrazolate, of a pyrazolyltriazenide chelating arm which completes the equatorial $CuN_4$ co-ordination. The centrosymmetric dinuclear units have intramolecular Cu · · · Cu distances of 3.852(5) and 3.839(4) Å respectively. The units are stacked in columns along the *b* axis. The cell also contains crossing channels filled with water molecules. The complex was characterized by spectroscopic and magnetic measurements. Magnetic susceptibility data show antiferromagnetic behaviour with an exchange parameter $|J| = 151$ cm$^{-1}$ significantly decreased with respect to symmetric doubly bridged complexes ($|J| = \approx 200$ cm$^{-1}$). The X-band powder EPR spectrum recorded at 77 K is typical of a triplet spin state lying above the singlet ground state. The results obtained for this complex are compared to recent literature data on other planar doubly bridged pyrazolate dicopper(II) complexes. A correlation, valid for symmetric as well as asymmetric systems, is described between the exchange parameter *J* and the deviation of the Cu–N–N bridge angle from the optimum value corresponding to the highest $|J|$.

The 1,3-bis(azolyl)triazenes are a family of compounds potentially able to form polynuclear complexes exhibiting interesting structures and properties. A large variety of co-ordination modes may be expected from the combination of the triazene group [1,2] and the azole [3] (triazole, pyrazole). Recently, we have shown that 1,3-bis[3-(5-amino-1,2,4-triazolyl)]triazene [4,5] (Hbatt) co-ordinates $Cu^{II}$ and $Pd^{II}$ in a tridentate mode involving the central nitrogen of the triazene group and one nitrogen of each triazole ring. The resultant complexes have the general formula [M(batt)X] (X = Cl, Br, I, NCS or CN).

1,3-Bis(pyrazol-3-yl)triazene ($H_2bpzt$) is another member of the bis(azolyl)triazene family. The present study is concerned with a complex of $Cu^{II}$ obtained with this compound. In principle, the change from aminotriazole to pyrazole affords a simpler situation regarding N-co-ordination possibilities and steric crowding on the heterocycles. It was interesting to examine whether tridentate co-ordination would also be adopted and whether the potential dinucleating ability of the pyrazole moiety would be effective. The compound $H_2bpzt$ can be viewed as a symmetrically substituted triazene or as an asymmetric pyrazole with a single chelating arm attached to the 3 position. In the latter view it presents unusual new features with respect to symmetric pyrazoles bearing chelating arms at the 3 and 5 positions, which have been intensively studied over the last years [6–13] for their dinucleating properties towards $Cu^{II}$.

In a recent report, Slangen *et al.*[14] have established a correlation between the value of the magnetic exchange parameter and the bridging geometry in planar dinuclear copper(II) complexes containing double 1,2,4-triazole-$N^1,N^2$ bridges. In particular the effect of the asymmetry of the bridging mode was clearly demonstrated in the case of the dinuclear doubly bridged complex $[Cu_2(pt)_2(SO_4)(H_2O)_3]\cdot 3H_2O$, in which Hpt is asymmetric 3-pyridin-2-yl-1,2,4-triazole. The study of the co-ordination of $Cu^{II}$ by $H_2bpzt$ affords the opportunity to examine the effect of an asymmetric bridging mode on the magnetic exchange parameter in a bis(μ-pyrazolato)-bridged dicopper complex. We report the synthesis, crystal structure and magnetic properties of the asymmetric dinuclear doubly bridged complex of $Cu^{II}$ with $H_2bpzt$. Also a correlation is proposed between the magnetic exchange parameter and the bridging angles to rationalize literature data on (quasi) planar bis(μ-pyrazolato)-bridged copper(II) complexes. A comparison is presented with the magnetostructural correlation recently established in the case of structurally related complexes containing ($N^1,N^2$) 1,2,4-triazole or triazolato bridges.[15]

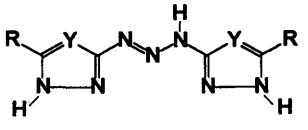

**Hbatt** Y = N, R = $NH_2$
**$H_2$bpzt** Y = CH, R = H

## Experimental

### Starting materials

3-Aminopyrazole (Acros Chimica) was distilled to a colourless

† For correspondence pertaining to the crystallographic studies.
*Non-SI unit employed:* eV ≈ 1.60 × 10$^{-19}$ J.

oil under reduced pressure (20 mmHg, *ca.* 2666 Pa; 157–162 °C). The other starting materials (p.a. grade, except methanol 99%) were used without further purification.

### Syntheses

**$H_2$bpzt.** The only available report of the synthesis of $H_2$bpzt refers to diazotization of 3-aminopyrazole in a concentrated phosphoric acid solution.[16] However, in our hands, this method proved to be irreproducible, giving only low yields. The synthesis was instead performed in dilute hydrochloric acid solution, with much better yields, as follows.

3-Aminopyrazole (5.4 g, 0.065 mol) was dissolved in 1% HCl (380 $cm^3$) and cooled to 0 °C. A solution of sodium nitrite (2.16 g, 0.031 mol) in water (30 $cm^3$) was added slowly to give a yellowish orange solution while maintaining the temperature around 0 °C. The compound began to precipitate immediately upon addition of a saturated solution of sodium acetate. After 15 min, $H_2$bpzt as a yellowish brown product was filtered off and washed with water, methanol, diethyl ether and finally dried at 85 °C overnight (3.14 g, 55%), m.p. 184–187 (decomp.) (Found: C, 40.6; H, 4.1; N, 55.3. $C_6H_7N_7$ requires C, 40.7; H, 4.0; N, 55.3%); *m/z* 177 ($M^+$, 10), 149 (12), 134 (13), 83 (100), 68 (17), 54 (16), 41 (19) and 28 (51%); $\tilde{\nu}_{max}/cm^{-1}$ 1596vs, 1566s, 1504m, 1470m, 1429vs, 1350m, 1331m, 1310s, 1256s, 1221m, 1190m, 1108s, 1067m, 937m, 787m, 754s and 732m; $\lambda_{max}/nm$ ($Me_2SO$) 332 ($\varepsilon/dm^3\ mol^{-1}\ cm^{-1}$ 14 300); $\delta_H$[200 MHz, $(CD_3)_2SO$, standard $SiMe_4$] 6.3 (s), 7.7 (s) and 12.3 (br).

**[{Cu(bpzt)}$_2$].** Two equivalents of potassium hydroxide (1.13 mmol, 3.11 $cm^3$ of a 0.363 mol $dm^{-3}$ methanolic solution) were added to $H_2$bpzt (100 mg, 0.565 mmol) dissolved in methanol (250 $cm^3$). To this orange-red solution, copper(II) chloride (96 mg, 0.563 mmol) dissolved in methanol (30 $cm^3$) was added with stirring; the solution turned dark brown. A few days later a brown needle-like product was separated from some amorphous material by several decantations and then filtered off, washed with methanol and ether. Yield 76 mg (56%) (Found: C, 30.2; Cu, 26.7; N, 40.7; O, 0.9. $C_{12}H_{10}Cu_2N_{14}\cdot 0.3H_2O$ requires C, 29.9; Cu, 26.3; N, 40.6; O, 1.0%). It has to be stressed that in most syntheses only a minute amount of small brown needles were formed. The predominant product was a polycrystalline material of much lower quality (shown to be the same complex by micro-Raman and Fourier-transform IR measurements). Although the Cu(bpzt) formula was never questioned for different syntheses, the elemental analyses gave various amounts of oxygen (0.9–6%), which in all cases remained below the 1.5 molecules of water per copper fixed by the structure determination (see Crystal structure section). Considering the role of water molecules in this structure, it is likely that the lack of part of the hydration water and the poor crystallinity of the predominant product are closely related.

### Physical measurements

Copper was determined by inductively coupled plasma analysis (Jobin-Yvon JY38 PLUS ICP). The analyses of the other elements were performed by Analytische Laboratorien, Professor Dr. H. Malissa and G. Reuter, Lindlar, Germany. The electron impact (EI) (70 ev) mass spectrum was recorded with a VG AutoSpec 6F Micromass instrument, the $^1$H NMR spectrum with a Bruker MSL200-15 spectrometer and electronic spectra with a Perkin-Elmer λ9 UV/VIS/NIR spectrophotometer. The IR spectra were recorded with a Bruker IFS 113 V Fourier–transform spectrophotometer, using KBr discs in the 4000–400 $cm^{-1}$ region and Nujol mulls between polyethylene windows below 400 $cm^{-1}$. Raman spectra of crystallites were recorded with a micro-Raman Mole S-3000 (Jobin-Yvon) instrument equipped with a 1420 B HQ photodiode array detector controlled by an OMA III system (EG&G Princeton Applied Research). The excitation radiation was the 514.5 nm line of a Spectra-Physics 2020 argon-ion laser. X-Band EPR spectra were recorded on a JEOL RE2x spectrometer. Magnetic susceptibilities were measured in the temperature range 20–285 K with a fully automated Manics DSM-8 susceptometer equipped with a TBT continuous-flow cryostat and a Drusch EAF 16 NC electromagnet, operating at *ca.* 1.4 T. Data were corrected for magnetization of the sample holder and for diamagnetic contributions, which were estimated from Pascal constants. Magnetic data were fitted by theoretical expressions minimizing the function $R = (\Sigma|\chi_{obs} - \chi_{calc}|^2/\Sigma|\chi_{obs}|^2)$.

### Crystallography

**Crystal data and data collection parameters.** $C_{12}H_{16}Cu_2N_{14}O_3$, $M = 531.46$, monoclinic, space group $P2_1/c$ (no. 14), $a = 12.899(8)$, $b = 6.714(5)$, $c = 24.286$ Å, $\beta = 119.98(5)°$, $U = 1822(2)$ Å$^3$ [by least-squares fitting of the setting angles of 11 well centred reflections (SET4[17]) in the range $6.2 < \theta < 12.1°$; the unit-cell parameters were checked for the presence of higher lattice symmetry[18]], $T = 150$ K, Mo-Kα radiation, $\lambda = 0.710\ 73$ Å, graphite monochromator, $Z = 4$, $D_c = 1.937(2)$ Mg m$^{-3}$, $D_m = 1.98(3)$ Mg m$^{-3}$, $F(000) = 1072$, brown, needle-shaped crystals with dimensions $0.03 \times 0.05 \times 0.4$ mm, $\mu$(Mo-Kα) = 2.39 mm$^{-1}$, no absorption correction applied, Enraf-Nonius CAD4-T diffractometer on rotating anode.

Four different crystals were tried before diffraction was observed. The measured crystal displayed extremely broad, unstructured reflection profiles of varying width (2.2–5.0°). Data were measured in ω-scan mode with scan angle $\Delta\omega = 2.25 + 0.35 \tan\theta°$. Intensity data were collected up to $\theta = 25.3°$ ($+h, -k, \pm l$). Only 10% of the intensity data were above $2.5\sigma(I)$ in the $\theta = 25°$ region. Data were corrected for 22% linear decay of one periodically measured reference reflection during 42 h of X-ray exposure time. Intensity data for 4704 reflections were measured, of which 3606 were independent ($R_{int} = 0.025$).

**Structure solution and refinement.** The structure was solved by automated Patterson methods and subsequent Fourier-difference techniques (DIRDIF 92[19]). Refinement on $F^2$ was carried out using full-matrix least-squares techniques (SHELXL 93[20]); no observance criterion was applied during refinement. Hydrogen atoms were included in the refinement in calculated positions riding on their carrier atoms. The positions of the oxygen atoms of the water molecules in the direct vicinity of a crystallographic inversion centre strongly suggested that their hydrogen atoms are disordered. The hydrogen atoms were placed according to a model allowing for all possible hydrogen bonds. These disordered hydrogen atoms were refined in a rigid group with the water oxygen as pivot atom, using mild distance restraints to maintain reasonable hydrogen-bond geometries. All non-hydrogen atoms were refined with anisotropic thermal parameters although restraints had to be applied to maintain reasonable anisotropy. The hydrogen atoms were included in the refinement with a fixed isotropic thermal parameter related to the value of the equivalent isotropic displacement parameter of their carrier atoms by a factor of 1.5 for the water hydrogen atoms and 1.2 for the other hydrogen atoms. The weighting scheme was $w^{-1} = \sigma^2(F^2) + (0.0515P)^2$, where $P = [\max(F_o^2,0) + 2F_c^2]/3$. The final $wR2$ $\{=[\Sigma w(F_o^2 - F_c^2)^2/\Sigma w(F_o^2)^2]^{\frac{1}{2}}\}$ was 0.214, $R1$ $(=\Sigma||F_o| - |F_c||/\Sigma|F_o|)$ was 0.107 [for 1087 $F_o > 4\sigma(F_o)$], $S = 0.99$, for 290 parameters and 264 restraints. Maximum $\Delta/\sigma = 0.16$. No residual density was found outside −0.95 and 1.17 e Å$^{-3}$ (near Cu). The relatively high $R$ values are related to the weak scattering that is most probably a consequence of the disorder in the solvent region. Geometrical calculations and illustrations were performed with PLATON.[21] All calculations were performed on a DEC5000 cluster. Selected bond distances and angles are given in Table 1.

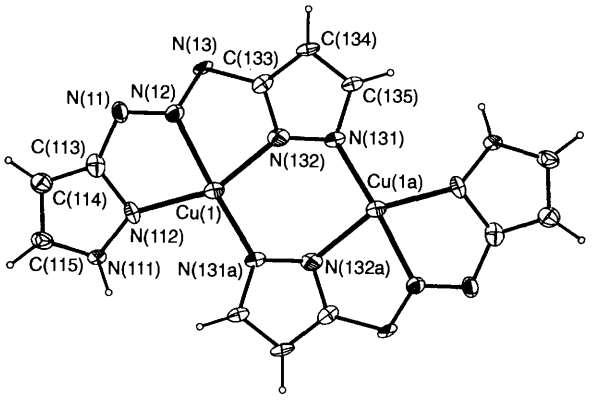


**Fig. 1** Thermal motion ellipsoid plot (probability level 50%)[21] of molecule 1 of [{Cu(bpzt)}$_2$] with atomic labelling

**Table 1** Selected bond distances (Å) and angles (°) for the two independent [{Cu(bpzt)}$_2$] molecules with estimated standard deviations in parentheses; $i$ = 1 or 2 refers to molecule 1 and 2, respectively*

| | Molecule 1 | Molecule 2 |
|---|---|---|
| Cu($i$)–N($i$12) | 2.003(19) | 1.950(19) |
| Cu($i$)–N($i$2) | 2.038(19) | 2.009(16) |
| Cu($i$)–N($i$32) | 1.981(16) | 1.95(2) |
| Cu($i$)–N($i$31a) | 1.911(17) | 1.959(16) |
| Cu($i$) · · · Cu($i$a) | 3.852(5) | 3.839(4) |
| N($i$31)–N($i$32) | 1.33(3) | 1.34(2) |
| N($i$2)–Cu($i$)–N($i$12) | 78.5(7) | 78.0(8) |
| N($i$2)–Cu($i$)–N($i$32) | 77.7(8) | 79.2(7) |
| N($i$32)–Cu($i$)–N($i$31a) | 98.9(7) | 99.2(7) |
| N($i$12)–Cu($i$)–N($i$31a) | 104.9(7) | 103.8(8) |
| N($i$12)–Cu($i$)–N($i$32) | 156.1(7) | 157.1(7) |
| N($i$2)–Cu($i$)–N($i$31a) | 176.4(7) | 175.9(6) |
| Cu($i$)–N($i$32)–N($i$31) | 138.3(13) | 139.5(14) |
| N($i$32)–N($i$31)–Cu($i$a) | 122.3(11) | 118.8(14) |
| Cu($i$)–N($i$12)–N($i$11) | 143.6(15) | 145.2(12) |
| N($i$1)–N($i$2)–N($i$3) | 121.0(18) | 120.7(16) |
| N($i$2)–N($i$1)–C($i$13) | 113.1(19) | 108.4(16) |
| N($i$2)–N($i$3)–C($i$33) | 107.2(16) | 111.0(16) |

* Atoms marked with a are obtained by applying the symmetry operation $-x, 2-y, -z$ (molecule 1) or $-x, 1-y, -z$ (molecule 2).

Atomic coordinates, thermal parameters and bond lengths and angles have been deposited at the Cambridge Crystallographic Data Centre (CCDC). See Instructions for Authors, *J. Chem. Soc., Dalton Trans.*, 1996, Issue 1. Any request to the CCDC for this material should quote the full literature citation and the reference number 186/236.

## Results and Discussion

### Crystal structure

The asymmetric unit contains two independent Cu(bpzt), each of which forms a dinuclear [{Cu(bpzt)}$_2$] complex situated at a crystallographic inversion centre. The monoclinic unit cell therefore contains four dinuclear units. A view of dinuclear unit 1 is shown in Fig. 1 with atomic labelling. The bpzt$^{2-}$ anion, deprotonated at the triazene [N(11) or N(13)] site and at the pyrazole [N(131)] site, acts as a 'tetradentate' ligand. The co-ordination mode is the combination of a tridentate chelating mode and a μ-pyrazolato bridging mode. The chelating mode involves the central nitrogen of the triazene group and two nitrogens of the azole groups. This nitro-type of co-ordination of the triazene group is uncommon and had not been observed until the report of complexes with Hbatt.[4,5] The tridentate chelation involving two joined five-membered rings accounts for the distorted square-planar co-ordination of the copper atom which presents two adjacent N–Cu–N angles as small as 78(1)°. The ligand and the whole molecule are nearly planar.

The dinuclear Cu(NN)$_2$Cu framework of molecule 1 is asymmetric as reflected by the difference between the Cu(1)–N(132)–N(131) and N(132)–N(131)–Cu(1a) angles which are 138.3(13) and 122.3(11)° respectively. The larger value of the first angle is a direct consequence of the rigidity of the pyrazoles which are substituents on the triazene group and are involved in the tridentate chelating mode. On the other hand, there is no such constraint upon the N(132)–N(131)–Cu(1a) angle. In the assembly of the two rigid Cu(bpzt) sub-units, the values of 122.3(11)° for this angle and of 98.9(7)° for the N(132)–Cu(1)–N(131a) angle appear to allow a fairly efficient overlap between the copper $d_{x^2-y^2}$ lobe of one sub-unit and the pyrazolic nitrogen σ orbital of the other one [N(131a)–Cu(1)–N(12) nearly collinear, small Cu(1)–N(131a) distance]. The Cu(bpzt) sub-units are not entirely rigid. The value of 138.3(13)° for the Cu(1)–N(132)–N(131) angle is reduced, caused by the formation of the dinuclear framework, as indicated by the Cu(1)–N(112)–N(111) angle of 143.6(15)° corresponding to the co-ordination by the outer pyrazole. There is clearly a compromise between this angular strain and the efficiency of the Cu–N overlap in the bridges. The final result is a nearly planar asymmetric Cu(NN)$_2$Cu framework, incorporating a Cu(1) · · · Cu(1a) distance of 3.852(5) Å.

The two crystallographically independent molecules, which are identical within experimental error, are stacked in a staggered way forming columns parallel to the $b$ axis (Fig. 2). A copper atom of one dinuclear framework lies approximately on top of a nitrogen atom of the other one, and *vice versa*. The two respective average planes are almost parallel with an angle of 3.4(4)°, but the intermolecular Cu · · · N distances are not equal [3.072(13), 3.201(14), 3.494(13) and 3.418(14) Å]. The least-squares planes through the molecules display acute angles of 70.23(10) and 73.00(10)° with the stacking $b$ axis for molecules 1 and 2 respectively.

Between the columns the structure contains a two-dimensional network of crossing channels filled with water molecules (12 $H_2O$ for four dinuclear units). The hydrogen atoms of these water molecules are disordered. There is extensive hydrogen bonding to and from this solvent region; pyrazole hydrogen (NH) as well as N(11) [N(21)] and N(13) [N(23)] of the triazene function are involved in hydrogen bonds with water molecules. The amount of oxygen accounted for by the structure determination, which is significantly above the value found by elemental analysis on powders, has been discussed in the Experimental section. This is in accord with the fact that the crystals easily lose water upon standing under ambient conditions.

### Infrared and Raman spectra

Correlations between the positions of the characteristic vibrations of the triazene group and the mode of co-ordination of this group have been established in the case of 1,3-diaryltriazenes.[2] However, the proposed rules concern the co-ordination through N$^1$ and (or) N$^3$ and are thus not applicable to the [{Cu(bpzt)}$_2$] complex in which the co-ordinating atom is N$^2$. We have performed isotopic substitution of the central nitrogen (N$^2$) in the ligand (using $Na^{15}NO_2$) and prepared [{Cu(bpzt)}$_2$] from this. Isotopic shifts ranging from 5 to 22 cm$^{-1}$ allowed the skeletal vibrations of the triazene group and the copper–triazene stretching mode to be assigned. The principal vibrational data for $H_2$bpzt and the complex are presented in Table 2.

Polarized micro-Raman measurements on oriented needles were also performed (experimental details are given elsewhere[5]). These measurements revealed a clear anisotropy of the polarizability tensor of the needles, the $\alpha_{xx}$ ($\alpha_{zz}$) component

**Table 2** Selected infrared and Raman data for $H_2$bpzt and its copper(II) complex[a]

| Compound | | $\nu_{asym}(N_3)$ | $\nu_{sym}(N_3)$ | $\delta(N_3)$ | $\nu_{breath}$ (triazole) | ν(M–N) triazene | ν(M–N) pyrazole |
|---|---|---|---|---|---|---|---|
| $H_2$bpzt | IR | 1429 (100) | 1256 (74) | 588 (14) | 1108 (82) | — | — |
| | Raman | [b] | | | | | |
| $[\{Cu(bpzt)\}_2]$ | IR | 1404 (100) | 1253 (sh) | 545 (10) | 1068 (14) | ≈391 (sh) | 351 (9) 309 (25) |
| | Raman | — | 1261 (100) | 552 (14) | 1066 (10) | 403 (4) | ≈344[c] |

[a] Wavenumber in $cm^{-1}$; relative intensities in parentheses. [b] The micro-Raman spectrum could not be recorded owing to fluorescence. [c] Very weak.

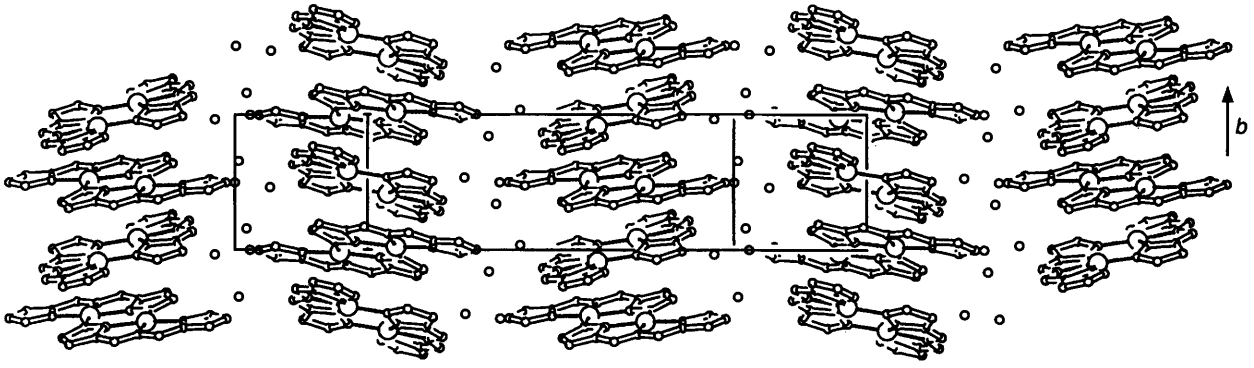


**Fig. 2** Crystal packing of $[\{Cu(bpzt)\}_2]\cdot 3H_2O$ showing the stacking of the dinuclear units (hydrogen atoms are omitted for clarity)

being much larger than the others (*y* is the needle axis), in particular in the case of the principal vibrations of the complex [$\nu_{sym}(N_3)$, $\nu_{breath}$(pyrazole), ν(Cu–N)]. This result is consistent with a columnar structure where nearly parallel copper–ligand units are stacked along the needle axis (see description of the structure).

### UV/VIS spectrum

The UV/VIS spectra were recorded for the complex as a mull in poly(chlorotrifluoroethylene) and as a solution in $Me_2SO$. The mull spectrum shows an intense and broad band at 482 nm and two bands of lower intensity at 310 and 252 nm. The more intense band extends into the whole visible region, preventing any analysis of the d–d transitions in the complex. Its absorption coefficient (in $Me_2SO$ solution) is of the order $10^4$ $dm^3$ $mol^{-1}$ $cm^{-1}$. This band can be assigned to the π–π* transition of the triazene group.[5] It is shifted to the red by 120 nm with respect to free $H_2$bpzt. This shift results from the delocalization of the deprotonated triazenide group and its conjugation with the pyrazole rings in the complex. The two bands of the complex in the UV region (310 and 252 nm) can be related to the band of free $H_2$bpzt at 230 nm (*cf.* band at 203 nm for vapour-phase pyrazole[22]). They are assigned to the π–π* transition of the two different pyrazole groups in $bpzt^{2-}$, the deprotonated bridging pyrazolate on the one hand and the terminal pyrazole on the other. In a $Me_2SO$ solution ($10^{-4}$ mol $dm^{-3}$) the UV/VIS bands of the complex are found at 420 and 283 nm (the third band is concealed by the strong $Me_2SO$ absorption at low wavelength).

### EPR spectrum

X-Band EPR spectra of a powdered sample have been recorded at room temperature and at 77 K. At room temperature only a broad signal was observed. However at 77 K, despite some mononuclear impurities, the spectrum is typical of dinuclear copper showing both $\Delta m_s = \pm 1$ and $\pm 2$ transitions[23] as depicted in Fig. 3. Depopulation of the triplet state upon cooling results in a significant decrease in intensity, but a better

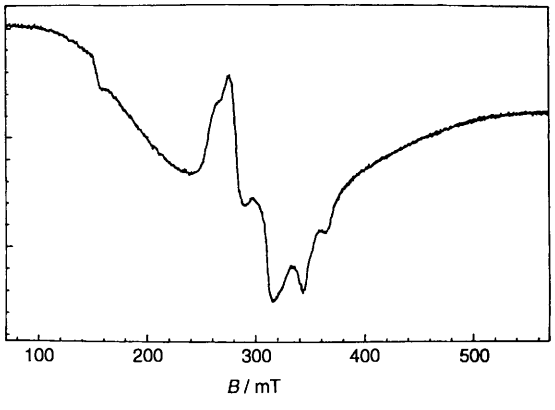


**Fig. 3** X-Band EPR spectrum of $[\{Cu(bpzt)\}_2]\cdot 3H_2O$ recorded at 77 K

resolution of the spectrum. At room temperature interactions between triplet-state molecules cause a broadening of the EPR lines. The half-field transition (forbidden $\Delta m_s = \pm 2$ transition) is not observed and the more intense triplet spectrum is no longer resolved.

### Magnetic properties

The magnetic susceptibility was recorded from 20 to 285 K (Fig. 4). The shape of the curve is typical of a dinuclear copper(II) complex with a strong antiferromagnetic coupling between the copper ions. The curve was fitted by the adapted Bleaney–Bowers[24] equation (1) for $S = \frac{1}{2}$ dimers where *p* represents the fraction of paramagnetic impurity [uncoupled copper(II) ions] and 2*J* the singlet–triplet gap defined by the spin Hamiltonian (2). The other parameters have their usual meanings. The best

$$\chi_m = (2N\beta^2g^2/kT)\,[3 + \exp(-2J/kT)]^{-1}\,(1 - p) + (N\beta^2g^2/2kT)\,p \quad (1)$$

$$H = -2J(S_1 \cdot S_2) \quad (2)$$

**Table 3** Magnetostructural parameters of (nearly) planar double pyrazolato-bridged copper(II) complexes[a]

| Compound[b] | $J$/cm$^{-1}$ | $d$/Å | | | Angle/° | | | Ref. |
|---|---|---|---|---|---|---|---|---|
| | | Cu · · · Cu | Cu–N | Cu′–N | N–Cu–N | Cu–N–N | Cu–N′–N′ | |
| $[Cu_2L^1{}_2][BPh_4]_2$ | −214 | 3.903 | 1.929 | 1.906 | 96.1 | 130.6 | 131 | 7 |
| $[Cu_2(bampz)_2Br_2]$ | −192 | 3.947 | 1.88 | 1.96 | 94.0 | 134 | 131 | 8 |
| $[Cu_2L^2{}_2(NO_3)(H_2O)]NO_3$[c] | −191 | 3.968 | 1.928 | 1.921 | 93.1 | 132.6 | 133.3 | 11 |
| | | | 1.930 | 1.933 | 93.2 | 133.2 | 133.1 | |
| $[\{Cu_2(bpypz)_2(H_2O)\}_2][NO_3]_2$ | −180.9 | 4.044 | 1.954 | 1.942 | 91.7 | 134 | 133.8 | 9 |
| $[Cu_2(H_2L)_2Cl_2]$ | −159 | 3.815 | 1.967 | 1.929 | 100.0 | 135.6 | 123.6 | 10 |
| $[Cu_2(bpzt)_2]$[d] | −151 | 3.852 | 1.98 | 1.91 | 98.9 | 138.3 | 122.3 | This |
| | | 3.839 | 1.95 | 1.96 | 99.2 | 139.5 | 118.8 | work |

[a] Clockwise notation CuNNCu′N′N′ for the atoms in the framework. [b] Hbampz = 3,5-Bis(aminomethyl)pyrazole; $HL^2$ = 3,5-bis(*N*-ethylamido)pyrazole; Hbpypz = 3,5-bis(pyridin-2yl)pyrazole; $H_3L$ = 1,1′-(4-methylpyrazole-3,5-diyl)diacetaldehyde dioxime. [c] Structural parameters of the two inequivalent bridges in the molecule. [d] Structural parameters of the two crystallographically independent molecules.

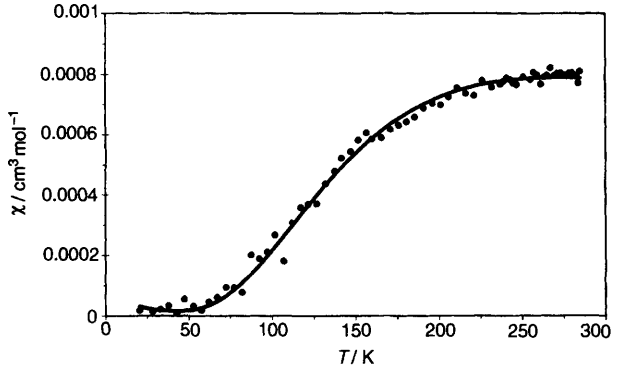


**Fig. 4** Temperature dependence of the magnetic susceptibility for $[\{Cu(bpzt)\}_2]\cdot 3H_2O$. The solid line represents the calculated curve ($J = -151$ cm$^{-1}$, $g = 2.13$, $p = 1.5 \times 10^{-3}$)

fit was obtained for the values $J = -151$ cm$^{-1}$, $g = 2.13$ and $p = 1.5 \times 10^{-3}$.

Magnetostructural correlations have been considered by Ajo *et al.*[6] using extended-Hückel molecular orbital (EHMO) calculations on $[Cl_2Cu(pz)_2CuCl_2]^{2-}$ as a model complex (pz = pyrazolate). These authors related the singlet–triplet energy gap to the angle formed by the two pyrazole planes and the angle formed by the two copper co-ordination planes. Calculations predict that the deviation from coplanarity of the two pyrazoles has the largest effect on the exchange interaction. Ajo *et al.*[6] recorded an experimental $J$ value of −120 cm$^{-1}$ for the complex $[PPh_4][\{H_2B(pz)_2\}Cu(pz)_2(Cl)Cu\{H_2B(pz)_2\}]$ in which the planes of the pyrazolate anions make an angle of 93° [$H_2B(pz)_2$ = dihydrobis(pyrazol-1-yl)borate]. In the case of the coplanar pyrazolate-bridged copper(II) complex $[Cu_2L^1{}_2][BPh_4]_2$ {$HL^1$ = 3,5-bis[2-(diethylamino)-ethylaminomethyl]pyrazole} Kamiusuki *et al.*[7] obtained a $|J|$ value of 214 cm$^{-1}$. This value which is the largest so far recorded can be expected to be close to the maximum for a pyrazolate doubly bridged copper(II) complex. Incidentally it would be interesting to measure the singlet–triplet energy gap of a new dinuclear copper(II) complex which presents an intermediary angle between the pyrazole planes (29.8°), as reported by Kumar *et al.*[12]

However, it appears from recent studies that dinuclear copper(II) complexes with coplanar pyrazolate bridges may have a smaller antiferromagnetic coupling constant (see Table 3). In particular, $[\{Cu(bpzt)\}_2]$ provides an example of an asymmetric pyrazolate-bridged system resulting in a reduced $|J|$ value (151 cm$^{-1}$). The asymmetry is a consequence of the structure of the ligand itself: $H_2$bpzt is an asymmetric pyrazole with a single chelating arm, which differs from the commonly reported symmetric chelating pyrazoles.[7–13]

If the difference between the Cu–N–N and Cu–N′–N′ angles is taken as a measure of the asymmetry, then it can be stated that $|J|$ decreases significantly with increasing asymmetry of the $Cu(NN)_2Cu$ framework (see Table 3). Triazole doubly bridged systems also show such a trend.[14] In this case, the decrease in $|J|$ was ascribed to a less effective overlap between the two copper magnetic orbitals, resulting from a larger asymmetry of the double diazene bridge (with possible relation to an enlargement of the N–Cu–N angle[15]).

General agreement exists that the dominant pathway for antiferromagnetic exchange in diazene-bridged systems is provided by σ bonding between copper $d_{x^2-y^2}$ and bridging ligand orbitals.[14,25–27] This suggests a natural correlation between the $J$ value and the Cu–N–N angle.[14,28,29] For the present discussion on dinuclear copper(II) di-μ-pyrazolate compounds, the structural parameters[7] of $[Cu_2L^1{}_2][BPh_4]_2$, which presents the highest $|J|$ value, will be taken as the optimum ones (Table 3). In the case of symmetrically (or nearly so) bridged complexes, $|J|$ decreases as the Cu–N–N angle increases (or the N–Cu–N angle decreases). In asymmetric systems, the Cu–N–N angles deviates from either side of the optimum angle and $|J|$ decreases markedly. Therefore, a convenient structural parameter to facilitate comparisons is the mean deviation defined as in equation (3) with $Cu–N–N_{opt}$

$$\delta(CuNN) = \tfrac{1}{2}(|CuNN - CuNN_{opt}| + |CuN'N' - CuNN_{opt}|) \quad (3)$$

130.8° for the series of planar complexes with double pyrazolate bridges.

When the $J$ values are plotted against δ(CuNN) for the series of compounds in Table 3 a quasi-linear relation is observed, at least in the symmetric case (see Fig. 5). Note that the complex $[NBu_4]_2[Cu_2(dcp)_2]$ (dcp = 3,5-dicarboxypyrazolate),[13] which has a $|J|$ value as low as 100 cm$^{-1}$, does not satisfy this relation. A tentative explanation might be that the two electron-withdrawing substituents on the pyrazole ring limit the exchange,[30] in a way similar to the electronegative $N^4$ atom in the $N^1$,$N^2$-triazole ring.[31]

The so-called optimum Cu–N–N angle for the pyrazolate-bridged complexes needs some comment. From simple considerations on bond geometry in a $Cu(NN)_2Cu$ framework,[15] it can be stated that Cu $d_{x^2-y^2}$–N σ overlap would ideally imply an N–Cu–N angle of 90° and a Cu–N–N angle of 126° for pyrazolate bridging. In a regular planar framework these requirements are incompatible and lead to two extreme situations, N–Cu–N 90 and Cu–N–N 135° on the one hand and N–Cu–N 108 and Cu–N–N 126° on the other. The compromise corresponds to N–Cu–N 99 and Cu–N–N 130.5°, values which are not too far from the optimum ones, corresponding to maximum $|J|$ (Table 3). In the same way, the six-membered pyridazine-bridged analogues would have optimum N–Cu–N and Cu–N–N angles close to 105 and 127.5° respectively.

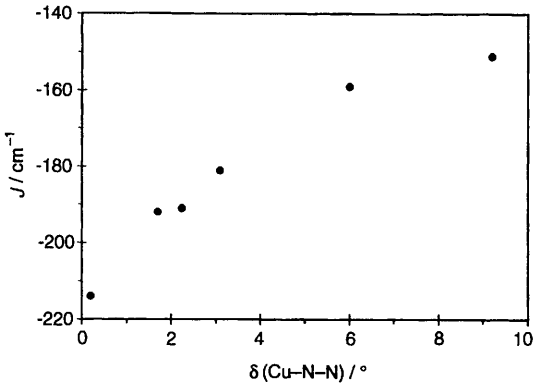


**Fig. 5** Variation of $J$ *vs.* δ(CuNN) [see equation (3)] for (nearly) planar pyrazolato doubly bridged copper(II) complexes

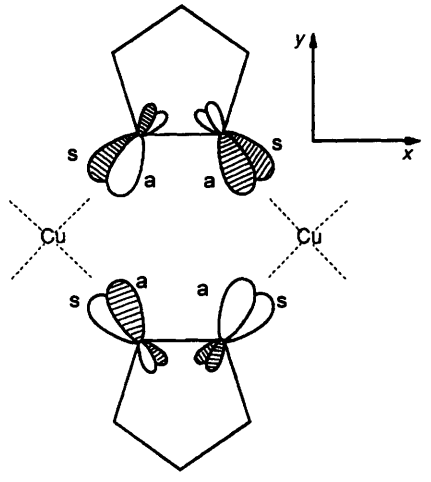


**Fig. 6** Schematic representation of the symmetric (s) and antisymmetric (a) HOMOs of the pyrazolate bridge in the dinuclear $Cu(pz)_2Cu$ framework (dashed crossed lines denote the corresponding symmetric and antisymmetric combinations of magnetic copper orbitals; symmetry refers to the mirror plane perpendicular to the N–N bond[6,32])

Although data on these complexes are quite scarce, it may be noted that a planar pyridazine doubly bridged complex with high $|J|$ value ($\approx 270$ cm$^{-1}$) has N–Cu–N and Cu–N–N angles of 105.5 and 127.1°.[29]

The different trend observed in the case of the doubly bridged triazole complexes is of interest:[15] the compound with the highest $|J|$ value has N–Cu–N and Cu–N–N angles of 90 and 135° respectively; moreover $|J|$ decreases almost linearly when N–Cu–N increases, in contrast to the case of the symmetric (or nearly symmetric) pyrazolate-bridged systems (Table 3). As in Fig. 5, the $J$ values for the triazole-bridged systems can also be correlated with a deviation parameter δ(CuNN) [equation (3)] with $Cu–N–N_{opt}$ 135°. This is of course equivalent to a plot of $J$ *vs.* N–Cu–N angle in the symmetric case, but a plot such as that in Fig. 5 may have the advantage of revealing a possible levelling effect at large asymmetry.

The angular dependence of superexchange in imidazolate[28] and pyrazolate-bridged systems[6,32] has been considered in the literature by using various molecular orbital exchange models.[30,33] In particular, it has been shown that the antisymmetric (symmetric) combination of the magnetic copper orbitals overlaps with an antisymmetric (symmetric) highest occupied molecular orbital (HOMO) of the pyrazolate bridge, which has a major contribution from the nitrogen $p_y$ ($p_x$) orbitals[6,32] (see Fig. 6). The energy difference between the two resulting antibonding MOs is related to the extent of antiferromagnetic coupling. The EHMO calculations performed for the $[Cl_2Cu(pz)_2CuCl_2]^{2-}$ model complex give an antisymmetric antibonding MO level which is higher than the symmetric one by an energy of 0.18 eV.[6]

On account of the (quasi) planarity of the $Cu(NN)_2Cu$ framework and the co-ordination around $Cu^{II}$, it may be reasonably assumed that the accessible range of Cu–N–N angles extends from about 125–130 to about 135–140° in a symmetric framework. Within this limited range it may be expected that, as the Cu–N–N angle increases, the overlap of the antisymmetric combination of the magnetic copper orbitals with the corresponding ligand HOMO decreases and the corresponding MO level becomes less antibonding (Fig. 6). At the same time the overlap of the symmetric orbitals should increase and the corresponding MO level should become more antibonding. Thus the $|J|$ value of symmetric doubly bridged pyrazolate complexes would be expected to decrease with increasing Cu–N–N angle. It may be noted that the opposite trend could be obtained in a bis(μ-diazene) complex series if the order of the two antibonding MOs could be reversed, the symmetric MO being higher in energy.

## Conclusion

For the first time, 1,3-bis(3-pyrazolyl)triazene ($H_2$bpzt), which has several potential co-ordination sites, has been studied with regard to its ligand properties. The synthesis, structure and magnetic properties of the copper(II) complex $[\{Cu(bpzt)\}_2]$ have been described. The complex has a dinuclear structure with an asymmetric double pyrazolato bridge, resulting in a magnetic interaction parameter $J$ of $-151$ cm$^{-1}$. With this result and recent literature data, the $J$ values of this and other species have been related to geometrical factors. As already emphasized in the case of triazole-bridged systems,[14] the absolute $J$ value decreases with the asymmetry of the $Cu(NN)_2Cu$ framework. On the other hand, $|J|$ decreases as the Cu–N–N angle increases in the symmetric case. With the aim of finding a magnetostructural correlation valid for the symmetric as well as for the asymmetric bridging geometry, we have considered as a structural parameter the mean deviation of the Cu–N–N angle with respect to the optimum angle (130.8°) corresponding to the complex with highest $|J|$. In this way, $J$ varies quasi-linearly with the angular deviation δ(CuNN). We propose that the origin of this relation lies in the orientation effect of the two pyrazole HOMOs on the splitting between the two antibonding MOs of the dinuclear unit. It is clear that a quantitative evaluation of the superexchange dependence on the Cu–N–N angle is required for more compounds to confirm this interpretation.

## Acknowledgements

One of us (V. P. H.) gratefully acknowledges the Belgian National Fund for Scientific Research (FNRS) for financial support and thanks Dr. P. Van Koningsbruggen (Leiden Institute of Chemistry) for helpful discussions. This work was supported in part by the Netherlands Foundation of Chemical Research (SON) with financial aid from the Netherlands Organization for Scientific Research (NWO) (to A. L. S.).

## References

1 D. S. Moore and S. D. Robinson, *Adv. Inorg. Chem. Radiochem.*, 1986, **30**, 1.
2 K. Vrieze and G. Van Koten, in *Comprehensive Coordination Chemistry*, eds. G. Wilkinson, R. D. Gillard and J. A. McCleverty, Pergamon, Oxford, 1987, vol. 1, pp. 195–206.
3 P. J. Steel, *Coord. Chem. Rev.*, 1990, **106**, 227.
4 V. Hanot and T. Robert, *J. Coord. Chem.*, 1994, **32**, 349.
5 V. Hanot, T. Robert and L. Vander Elst, *Synth. React. Inorg. Metal-Org. Chem.*, 1994, **24**, 1191.
6 D. Ajo, A. Bencini and F. Mani, *Inorg. Chem.*, 1988, **27**, 2437.
7 T. Kamiusuki, H. Okawa, N. Matsumoto and S. Kida, *J. Chem. Soc., Dalton Trans.*, 1990, 195.

8 T. Kamiusuki, H. Okawa, H. Inoue, N. Matsumoto, M. Kodera and S. Kida, *J. Coord. Chem.*, 1991, **23**, 201.
9 J. Pons, X. Lopez, J. Casabo, F. Teixidor, A. Caubet, J. Rins and C. Miravitlles, *Inorg. Chim. Acta*, 1992, **195**, 61.
10 B. Mernari, F. Abraham, M. Lagrenee, M. Drillon and P. Legoll, *J. Chem. Soc., Dalton Trans.*, 1993, 1707.
11 F. Degang, W. Guoxiong, Z. Zongyan and Z. Xiangge, *Transition Met. Chem.*, 1994, **19**, 592.
12 M. Kumar, V. J. Aran, P. Navarro, A. Ramos-Gallardo and A. Vegas, *Tetrahedron Lett.*, 1994, **31**, 5723.
13 J. C. Bayon, P. Esteban, G. Net, P. G. Rasmussen, K. N. Baker, C. W. Hahn and M. M. Gumz, *Inorg. Chem.*, 1991, **30**, 2572.
14 P. M. Slangen, P. J. Van Koningsbruggen, K. Goubitz, J. G. Haasnoot and J. Reedijk, *Inorg. Chem.*, 1994, **33**, 1121.
15 P. J. Van Koningsbruggen, Ph.D. Thesis, Leiden University, 1994.
16 H. Reimlinger, A. Van Overstraeten and H. G. Viehe, *Chem. Ber.*, 1961, **94**, 1036.
17 J. L. Boer and A. J. M. de Duisenberg, *Acta Crystallogr., Sect. A*, 1984, **40**, C410.
18 A. L. Spek, *J. Appl. Crystallogr.*, 1988, **21**, 578.
19 P. T. Beurskens, G. Admiraal, G. Beurskens, W. P. Bosman, S. Garcia-Granda, R. O. Gould, J. M. M. Smits and C. Smykalla, the DIRDIF program system, Technical report of the Crystallography Laboratory, University of Nijmegen, 1992.
20 G. M. Sheldrick, SHELXL 93, Program for crystal structure refinement, University of Göttingen, 1993.
21 A. L. Spek, *Acta Crystallogr., Sect. A*, 1990, **46**, C34.
22 J. Elguero, in *Comprehensive Heterocyclic Chemistry*, ed K. T. Potts, Pergamon, Oxford, 1984, vol. 5, part 4A, pp. 197–199.
23 A. Bencini and D. Gatteschi, *EPR of Exchange Coupled Systems* Springer, New York, 1990, pp. 173–187.
24 B. Bleaney and K. D. Bowers, *Proc. R. Soc. London, Ser. A*, 1952 **214**, 451.
25 O. Kahn, *Inorg. Chim. Acta*, 1982, **62**, 3.
26 M. S. Haddad, S. R. Wilson, D. J. Hodgson and D. N. Hendrickson *J. Am. Chem. Soc.*, 1981, **103**, 384.
27 G. Kolks, S. J. Lippard, J. V. Warzczak and H. R. Lilienthal, *J. Am. Chem. Soc.*, 1982, **104**, 717.
28 A. Bencini, C. Benelli, D. Gatteschi and C. Zanchini, *Inorg. Chem.*, 1986, **25**, 398.
29 F. Abraham, M. Lagrenee, S. Sueur, B. Mernari and C. Bremard, *J. Chem. Soc., Dalton Trans.*, 1991, 1443.
30 P. J. Hay, J. C. Thibeault and R. H. Hoffmann, *J. Am. Chem. Soc.*, 1975, **97**, 4884.
31 S. S. Tandon, L. K. Thompson and R. C. Hynes, *Inorg. Chem.*, 1992, **31**, 2210.
32 Y. Nishida and S. Kida, *Inorg. Chem.*, 1988, **27**, 447.
33 O. Kahn, *Angew. Chem., Int. Ed. Engl.*, 1985, **24**, 834.

*Received* 28*th March* 1996; *Paper* 6/02181F